The critical end point of QCD

Sourendu Gupta
(TIFR, Mumbai)

SEWM 2006, BNL

13 May, 2006

The conjectured phase diagram, Taylor expansion of the pressure, the sources of systematic uncertainties, estimate of the critical end point.

Plan

1. An introduction to the phase diagram of QCD and modern methods for computing at finite chemical potential

2. The technique of analytic continuation of the free energy by the method of Taylor expansion around vanishing chemical potential

3. Estimating the critical end point of QCD and the wing critical line in the QCD phase diagram

4. The physical degrees of freedom in the plasma phase of QCD: the evidence from linkage and screening correlators.

Global symmetries determine the phase diagram

Two flavours of light quarks: approximate $SU(2) \times SU(2)$ chiral symmetry, in the limit broken spontaneously to diagonal $SU(2)$, (pseudo) Goldstone bosons are the (light pseudo-scalar) pions.

Five tunable parameters: T (temperature), μ_u and μ_d (two chemical potentials), m_u and m_d (two masses). Gibbs phase rule allows large order multi-critical points.

Order parameter for chiral symmetry restoration: $\langle \overline{\psi}\psi \rangle$, tuned by changing T and $\mu = (\mu_u + \mu_d)/2$, excitations in this "radial" direction are heavy scalar mesons.

Order parameter for pion condensation: $\langle \overline{\psi}\gamma_5\tau_2\psi \rangle$, non-zero value may be induced by tuning isospin chemical potential $\mu_3 = (\mu_u - \mu_d)/2$, excitations in this direction give a massless charged pion.

The phase diagram

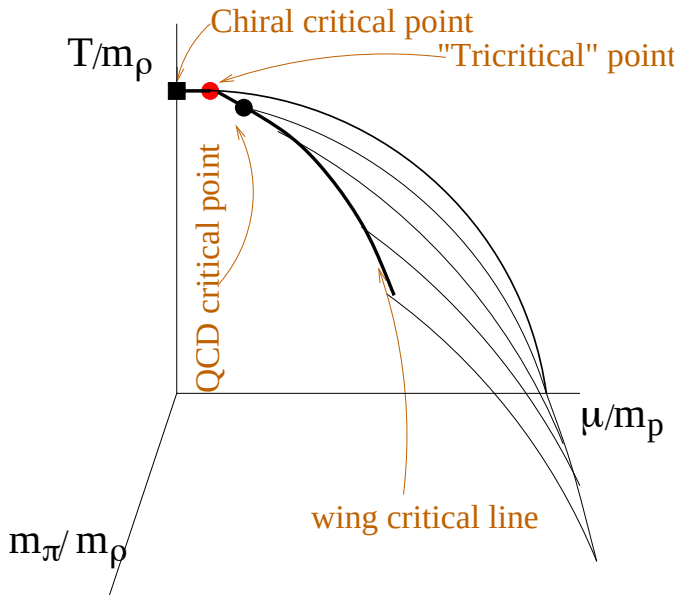

Berges and Rajagopal
Halasz, Jackson, Schrock, Stephanov and Verbaarschot
1998

Section of the 5-d phase diagram along a surface of $\mu_3 = 0$ and $m_u = m_d$: phases distinguished by $\langle\overline{\psi}\psi\rangle$. Other interestingly ordered phases at larger μ.

The sign problem

$$Z = \mathrm{e}^{-F(T,\mu)/T} = \int DU\ \mathrm{e}^{-S} \prod_f \det M(U, m_f, \mu_f)$$

where the Dirac operator is a lattice discretisation of $M = m + \partial_\mu \gamma_\mu$.

- If there is a Q such that $M^\dagger = Q^\dagger M Q$, then clearly $\det M$ is real.
- $Q = \gamma_5$ for $\mu = 0$. Nothing for $\mu \neq 0$. Monte Carlo simulations of Z fail.
- Thermodynamics remains valid, free energy is fine.

Developing methods to work with the sign problem

- Reweighting: Simulate at some parameter set, reweight the Fermion determinant (M, inside the path integral) to another parameter set. Fodor and Katz (hep-lat/0104001) used density of states method, Bielefeld-Swansea (hep-lat/0204010) used Taylor expansion of determinant.
- Analytic continuation: Find F and derivatives at some parameter set, make analytical continuation of F (outside the path integral) to another parameter set.
  - Imaginary chemical potential: $\exp(i\mu)$ like a $U(1)$ gauge field, no sign problem. de Forcrand and Philipsen (hep-lat/0205016), d'Elia and Lombardo (hep-lat/0209146) used regular imaginary μ, Azcoiti et al (hep-lat/0409157) extended to two couplings.
  - Taylor Expansion of free energy: Gavai and SG (hep-lat/030301), Bielefeld-Swansea (hep-lat/0305007)

The Taylor expansion of the pressure for 2 flavours

$$P(T,\mu_u,\mu_d) = \left(\frac{T}{V}\right) \log Z(T,\mu_u,\mu_d)$$

$$P(T,\mu_u,\mu_d) = P(T,0,0) + \sum_{n_u,n_d} \chi_{n_u,n_d} \frac{\mu_u^{n_u}}{n_u!} \frac{\mu_d^{n_d}}{n_d!}$$

$m_u = m_d$ implies that $\chi_{n_u,n_d} = \chi_{n_d,n_u}$, for any $\mu_u = \mu_d$. One QNS is

$$\chi_B(T,\mu_B) = \left.\frac{\partial^2 P(T,\mu_u,\mu_d)}{\partial \mu_B^2}\right|_{\mu_u=\mu_d=\mu_B/3}$$

$\chi_B(T^E,\mu_B^E)$ diverges in the infinite volume limit: pseudo critical behaviour at finite volumes. van Hove's theorem

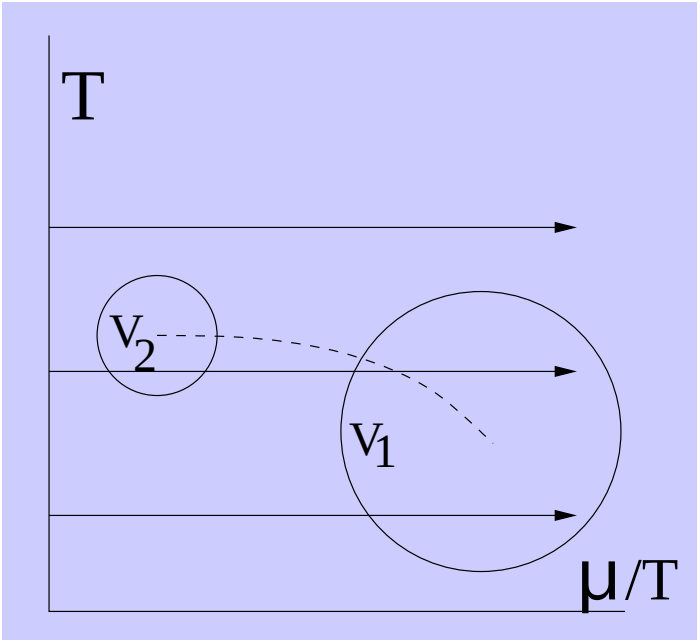

Differential calculus by machine: 1

There are mechanical and (almost) fully programmable methods to take the derivatives involved in a high-order Taylor series expansion of the partition function with fermions and finding the most efficient way of programming the Taylor coefficients.

Step 1

Relate the derivatives of $\log Z$ to the derivatives of Z. Trivially accomplished by, *e.g.*, the simple Mathematica program

$$\texttt{chi[n\_, m\_]} := \texttt{D[Log[Z[u, d]], \{u, n\}, \{d, m\}],}$$

or its generalization to a larger number of flavours. Notation used is

$$\chi_{nm} = \chi_{\underbrace{uu\cdots}_{n\,times}\,\underbrace{dd\cdots}_{m\,times}}$$

Differential calculus by machine: 2

Step 2

Relate the derivatives of Z to fermion traces. As long as we work with equal mass flavours, the fermion traces are flavour independent. Introduce the notation

$$Z_{10} = Z\langle \mathcal{O}_1 \rangle, \qquad \mathcal{O}'_n = \mathcal{O}_{n+1}.$$

Use the rule $[\det M]' = [\exp \mathrm{Tr}\, \log M]' = \mathrm{Tr}\, M' M^{-1} \det M$, to write

$$Z_{10} = Z_{01} = \frac{\partial Z}{\partial \mu_f} = \int DU \mathrm{e}^{-\mathcal{S}}\, \mathrm{Tr}\, M_f^{-1} M'_f.$$

Note: $M' = \gamma_0$ and $M^{-1} = \psi\overline{\psi}$, so $\mathrm{Tr}\, M^{-1} M' = \psi^\dagger \psi$.
S. Gottlieb *et al.*, *Phys. Rev. Lett.*, 59 (1987) 2247

Differential calculus by machine: 3

Step 3

Use the chain rule to write down higher order derivatives in terms of the $\mathcal{O}_n$ and their products. A diagrammatic representation of these quantities is possible, and can be used to check the results. SG, Zakopane lectures, 2002

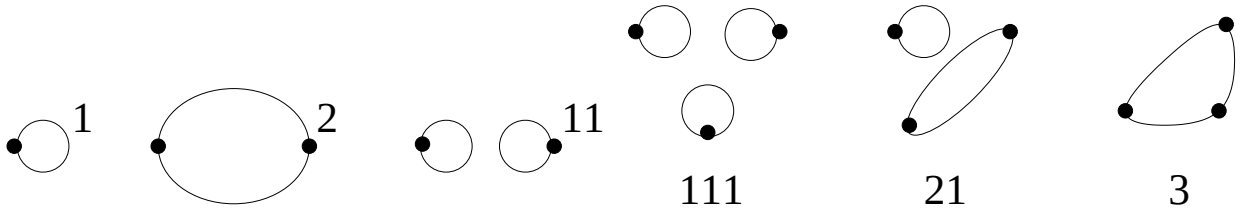

Example: Z_{60} contains $\mathcal{O}_{1122}$ with coefficient equal to the number of ways of partitioning 6 objects into groups of 2 ones and 2 twos, i.e.,

$$\left\{\frac{1}{2}\binom{6}{1}\binom{5}{1}\right\} \times \left\{\frac{1}{2}\binom{4}{2}\right\} = 45.$$

Differential calculus by machine: 4

Step 4

The diagrams still have to be related to fermion traces. In the continuum this is trivial because only $M' = \gamma_0 \neq 0$. On the lattice there are several more steps, since arbitrary derivatives, $M^{(p)}$, exist. Introduce further notation

$$\lfloor n_1 \cdot p_1 \oplus n_2 \cdot p_2 \oplus \cdots \rceil = \mathrm{Tr}\left[\left(M^{-1}M^{(p_1)}\right)^{n_1}\left(M^{-1}M^{(p_2)}\right)^{n_2}\cdots\right].$$

Then derivatives are given by the rule—

$$\lfloor n \cdot p \rceil' = -n\lfloor 1 \oplus n \cdot p\rceil + n\lfloor (n-1)\cdot p \oplus (p+1)\rceil.$$

The chain rule is equivalent to making the derivative linear over $\oplus$.

Example: $\lfloor 1\rceil = \mathrm{Tr}\, M^{-1}M'$, and $\lfloor 1\rceil' = -\lfloor 2\cdot 1\rceil + \lfloor 2\rceil$.

Differential calculus by machine: 5

Step 5

Numerical estimates of traces are made by the usual noisy method, which involves the identity $I = \overline{|r\rangle \langle r|}$, where r is a vector of complex Gaussian random numbers. We need upto 500 vectors in the averaging.

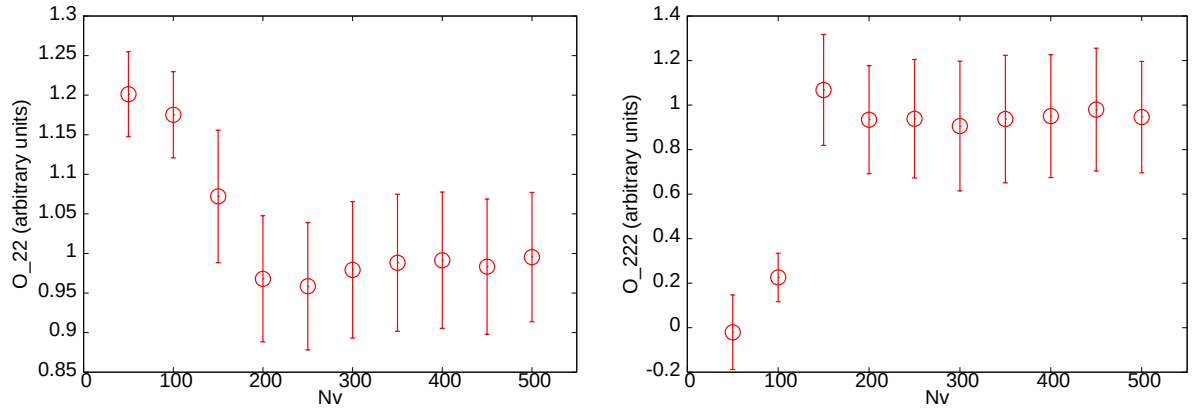

Central value: measurement with exactly N_v vectors; bars: config-to-config variation. Statistics of vectors (N_v) is the big issue. Statistics of configs secondary. Bielefeld: $N_v = 50$–100, Mumbai: $N_v = 400$–500.

Differential calculus by machine: 5

Step 5: why so many vectors?

Distribution of each trace is Gaussian. Product of traces such as χ_{2222} strongly non-Gaussian. Proof: For a Gaussian random number of unit variance

$$\langle x_i^2 \rangle = 1, \qquad \langle x_i^4 \rangle = 3 \qquad \text{implies } \left[x_i^4\right] \equiv \langle x_i^4 \rangle - 3\langle x_i^2 \rangle^2 = 0,$$

but for a product of independent Gaussian numbers $v = x_1 x_2 \cdots x_n$,

$$\langle v^2 \rangle = 1, \qquad \langle v^4 \rangle = 3^n \qquad \text{implies } \left[v^4\right] = 3^n - 3.$$

The distribution of v can be written down in closed form in special cases.

Central limit theorem applies: distribution of $\overline{v}$ is Gaussian (proof straightforward). But to reduce the 4th cumulant to substantially below the 2nd, one needs statistics $\gg 3^n$. So, the number of vectors $N_v \gg \mathcal{O}(n3^n)$.

Differential calculus by machine: 6

Step 6

Optimisation of the computation of multiple traces reduces to an NP-complete problem in computer science called the Steiner problem. Need 20 matrix inversions to perform a single measurement of upto 8th order susceptibilities.

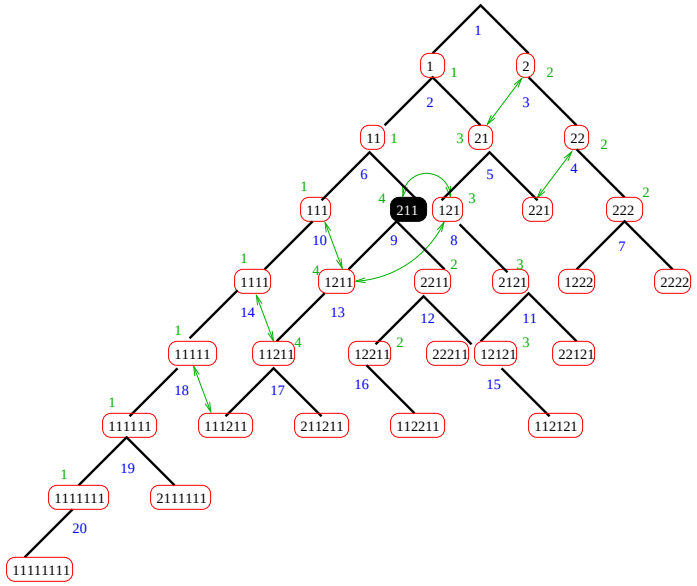

Note the accuracy checks built into the optimal computation.

Fluctuations

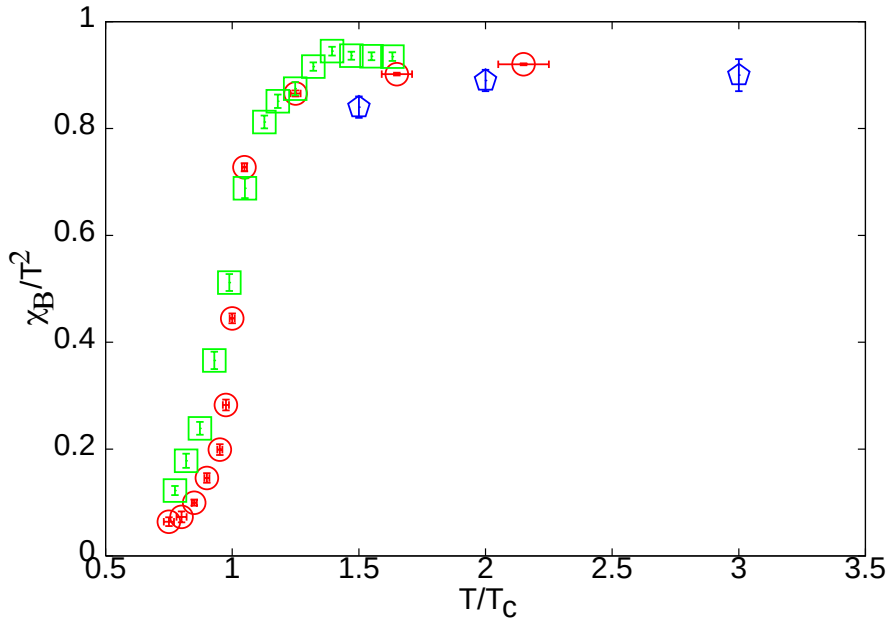

Quenched continuum (Mumbai), MILC $a = 1/8T$, $N_f = 2$, Mumbai $N_f = 2$ continuum extrapolation through quenched

Weak coupling expansion: Blaizot, Iancu and Rebhan, Vuorinen

4th order NLS peaks at T_c

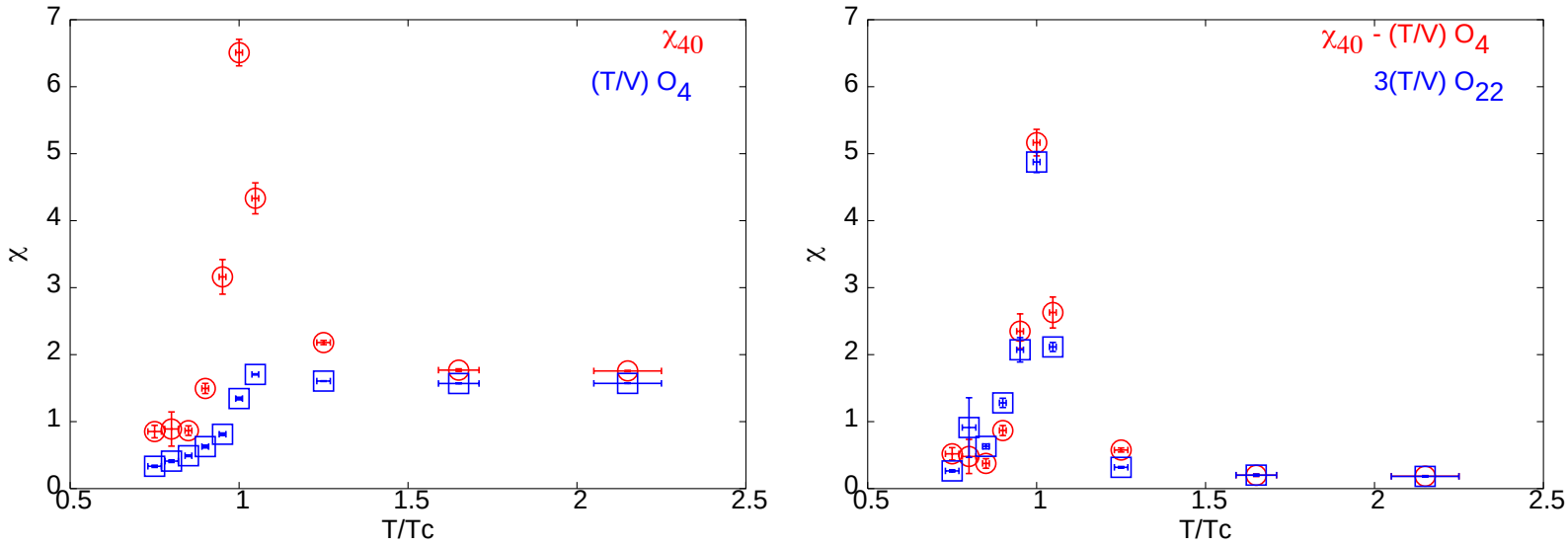

Peak due to multiloop operators: correspond to products of traces.

Proper control of $(T/V)\langle O_{22}\rangle$ is needed to obtain the correct value of χ_{40} (and χ_{22}) near T_c. Similiar control of products of traces needed for all higher susceptibilities in this region.

Proper choice of N_v crucial.

Quark mass dependence

Radius of convergence: $\mu^*/T = \sqrt{|12\chi_B^{(2)}/\chi_B^{(4)}|}$.

Peak in χ_{40} implies decreasing radius of convergence. The radius of convergence seems to be very sensitive to quark mass in a region near T_c. Interpolation to $m_\pi/m_\rho = 0.7$ is consistent with the break point in Bielefeld-Swansea result.

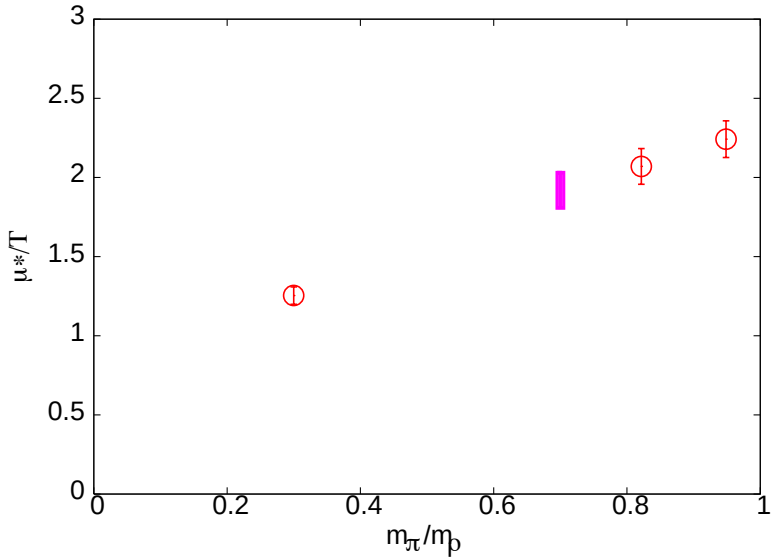

Partially quenched computation. Sea quarks correspond to the lowest mass shown here.

The wing critical line

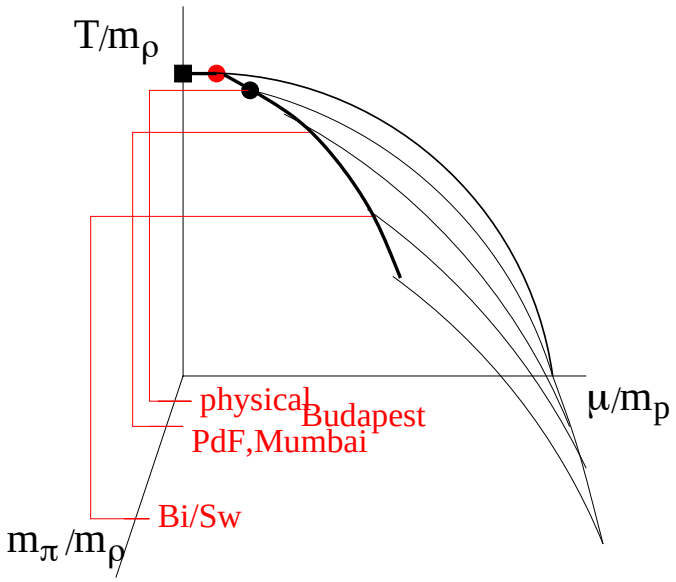

How curved is the wing critical line? Data from different simulations can be combined to answer this question since they are at similiar values of m_p/m_ρ but different m_π/m_ρ. Criticality may be harder to observe at larger m_π/m_ρ, but simulations are easier.

Theorems on series analysis

Fundamental theorem If the series expansion of an analytic function in one complex variable has a radius of convergence ρ, then there is at least one singular point on the circle of radius ρ centered on the point at which the expansion is constructed.

Singular point is one where the function is not analytic (although it may have a value at that point).

Example 1: the series for pressure can have a finite radius of convergence. The value of pressure at the singular point is well defined, although its derivatives do not exist.

Example 2: the series for the susceptibility may have a finite radius of convergence. Usually, even the value of this function does not exist at a singular point on the circle at the boundary of convergence.

Where is the singular point?

If all the coefficients of the series are positive then the singular point lies on the positive real axis.

If there is a pattern to the number of negative coefficients separating successive positive coefficients, then one can deduce the phase angle of the singular point.

Example 1: alternating series; singularity on negative real axis.

Example 2: The series expansion of

$$\frac{1}{1+\exp(i\theta)z}+\frac{1}{1+\exp(-i\theta)z}=2+2\cos\theta z+2\cos 2\theta z+2\cos 3\theta z^3+\cdots,$$

has sign changes dictated by the value of θ.

Radius of convergence and divergence of series

Take a partial sum of the series—

$$f_n(x) = \sum_{i=0}^{n} f_i x^i,$$

such that it has a radius of convergence ρ. This sum need not diverge at the radius of convergence. The only signal of the divergence is that partial sums for different n differ increasingly more for $|x| > \rho$.

Example 1: The series $\sum x^i/i$ diverges at $x = 1$, but all partial sums are perfectly well behaved across $x = 1$—

$$1 + x, \quad 1 + x + x^2/2, \quad 1 + x + x^2/2 + x^3/3, \cdots$$

Radius of convergence and divergence of series

Example 2: The series for the magnetic susceptibility of the two dimensional Ising model in $y = \exp(-2\beta H)$ around $y = 0$ has unit radius of convergence but the partial sums are perfectly smooth and well behaved. The exact ratio $m/\chi = 0$ in the ordered phase, but the partial sums are perfectly smooth across $y = 1$.

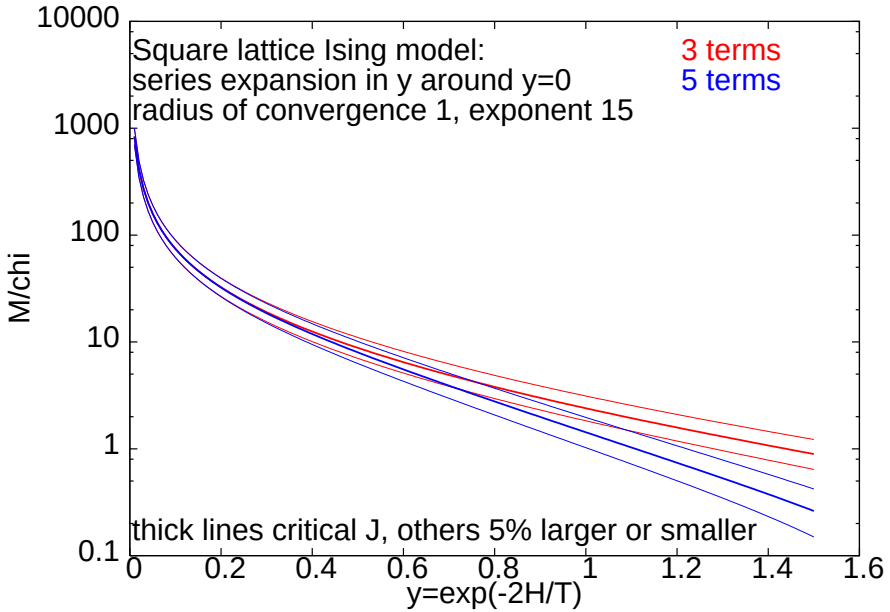

Radius of convergence and divergence of series

Example 3: In QCD, the partial sums of the series for χ_{20} are perfectly smooth. The ratio n_B/χ_B is also perfectly smooth and non-zero at the radius of convergence. Allton et al., *Phys. Rev.* D 71 (2005) 054508

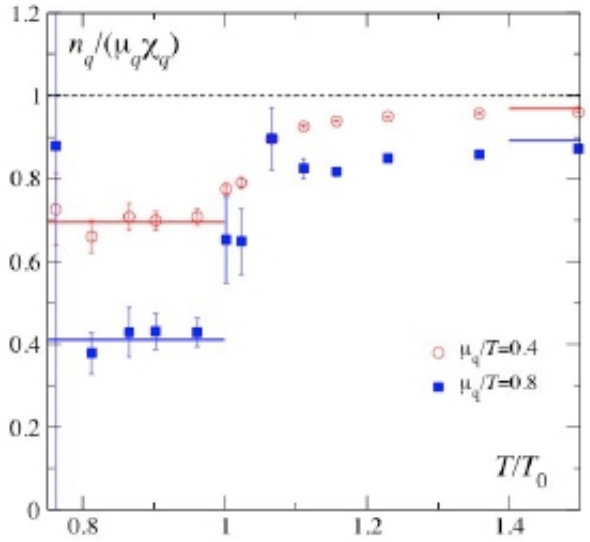

Series coefficients in QCD

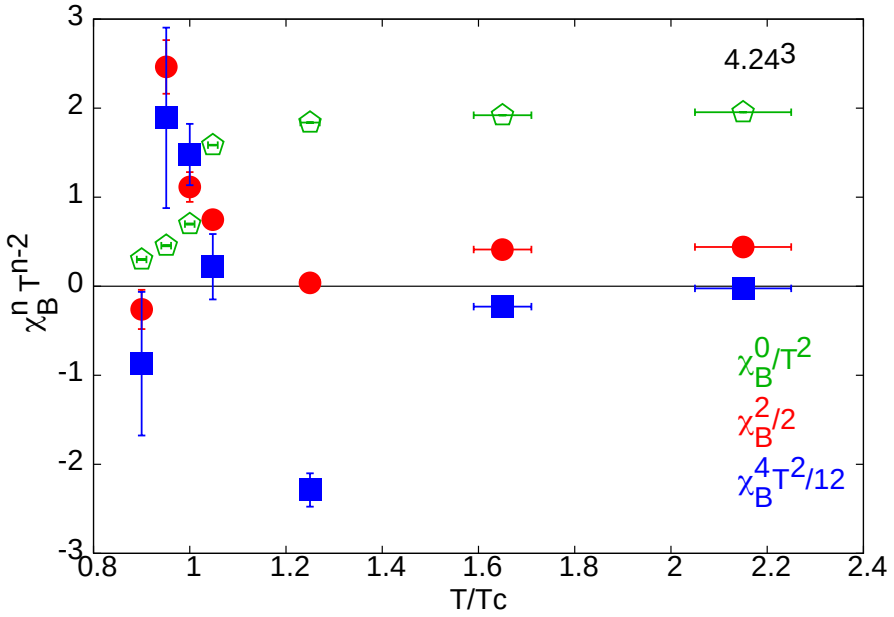

Between $T = 0.95T_c$ and $T = 0.9T_c$ the singularity moves off the real μ axis. Hence the critical end point is bracketed between these two temperatures. We have quoted $T^E \simeq 0.95T_c$.

Radius of convergence

Notation: If $f(x) = \sum_n f_{2n} x^{2n}$ then $\rho_{2n} = \left|\frac{f_0}{f_{2n}}\right|^{1/2n}$ and $r_{2n+1} = \sqrt{\left|\frac{f_{2n}}{f_{2n+2}}\right|}$

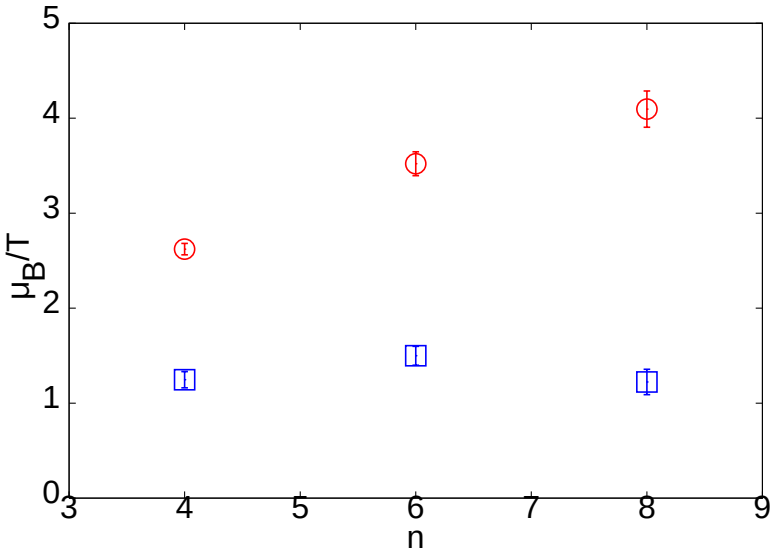

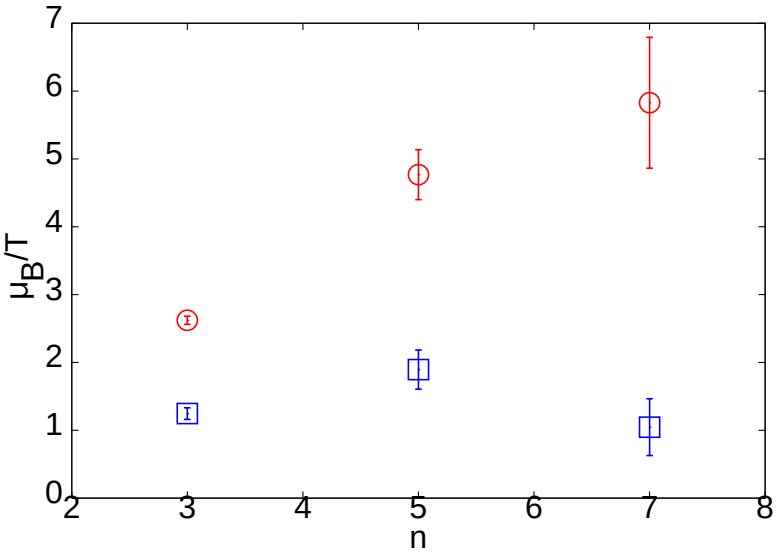

Old Budapest results roughly consistent with our small volume analysis. A threshold $Lm_\pi \approx 5$ is needed to study the thermodynamic limit.

The QCD critical end point

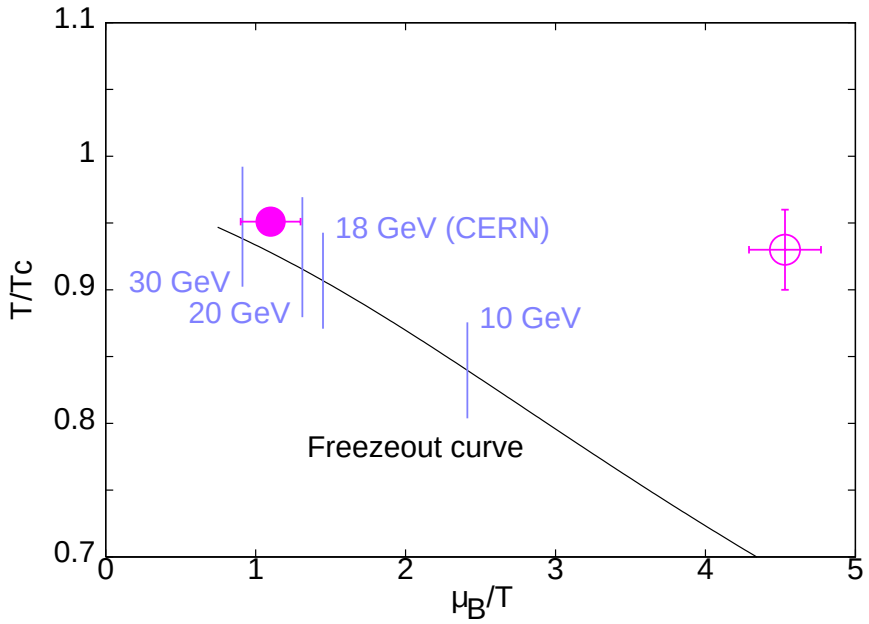

R. V. Gavai and SG, PRD 71 (2005) 114014

Strong finite volume effect; strong quark mass effect. When $Lm_\pi \to \infty$, $a = 1/4T$ and $m_\pi/m_\rho = 0.3$ then $T^E/m_\rho \approx 0.17$ and $\mu^E/m_\rho \approx 0.19$.

What to control in a reliable computation

1. Statistics of random vectors: $N_v \simeq 400$–700 required. One test: off-diagonal higher order susceptibilities must be independent of lattice volume.
2. Statistics of configurations: secondary problem. All configurations should be statistically independent, otherwise systematic effects. Measure autocorrelation times (τ). Statistical errors: $\sigma^2_{actual} = (1 + 2\tau)\sigma^2_{apparent}$.
3. Spatial volume: must be large enough to contain more than 5 Compton wavelengths of the pion. Even larger if one wants to study critical indices.
4. Quark mass is crucial. State of the art is a quark mass such that m_π/m_ρ is 50% larger than the physical value.
5. Lattice spacing errors currently undetermined. Require two computations at the same m_π/m_ρ with two actions having different lattice spacing effects.

Summary of phase diagram

1. Sign problem under reasonable control in QCD for $T/m_\rho > 0.13$.

2. Taylor expansion can be used to explore the phase diagram upto the nearest singularity to the $\mu = 0$ starting point.

3. Extrapolation to infinite volume has pitfalls: careful. Need N_v large, control over τ and $Lm_\pi \geq 5$.

4. With $a = 1/4T$ and $m_\pi/m_\rho = 0.3$ one finds $T^E/m_\rho \approx 0.17$ and $\mu^E/m_\rho \approx 0.20$.

5. Strong dependence on quark mass, i.e., m_π/m_ρ.

Quasiparticles: linkage of quantum numbers

Identify a particle by a complete set of quantum numbers. When there are many conserved quantum numbers the problem is simple. Look at two quantum numbers simultaneously— say U and D.

$T = 0$: whenever $U = 1$ is excited $D = -1$ is excited along with it.

$T > T_c$: when $U = 1$ is excited $D = \pm 1$ should be excited along with it if the medium contains quarks. Otherwise, by observing what value of D is preferentially excited, you find something about the quantum numbers of the excitations.

Similarly one could study the linkages $U|B$ or $U|Q$, or $D|B$ etc.

$$C_{(XY)/Y} \equiv \frac{\langle XY \rangle - \langle X \rangle \langle Y \rangle}{\langle Y^2 \rangle - \langle Y \rangle^2} = \frac{\chi_{XY}}{\chi_Y}$$

Linkage is robust

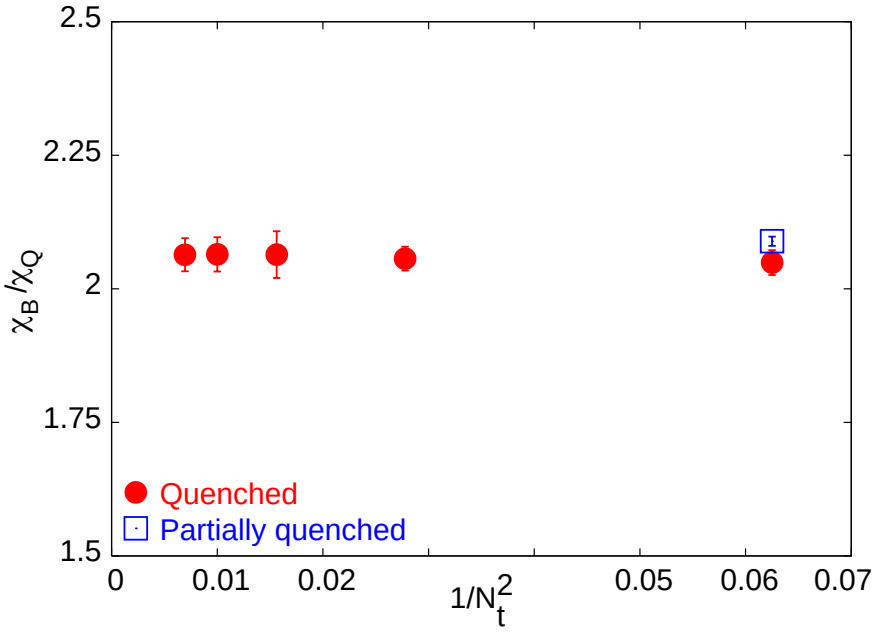

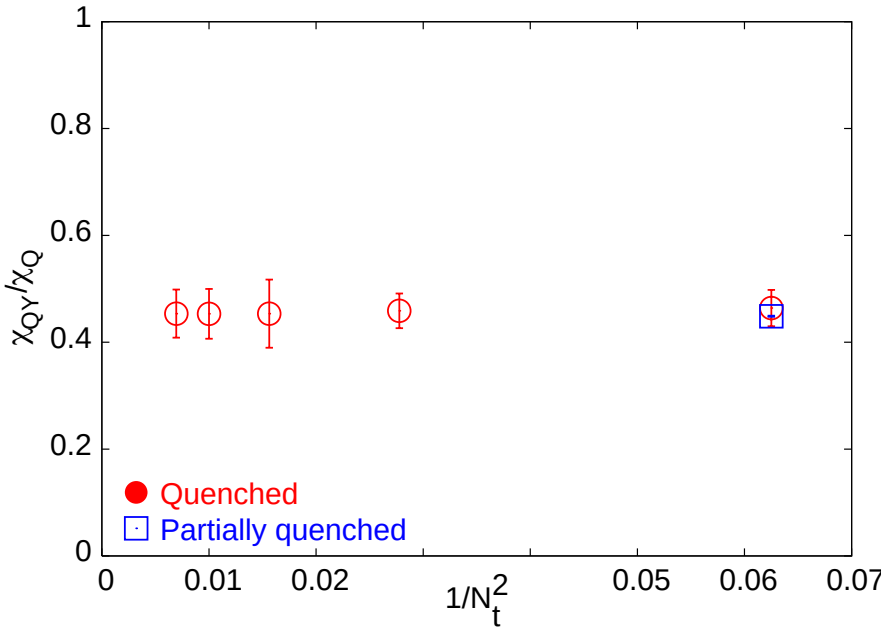

Above T_c ratios of QNS are almost independent of lattice spacing, and insensitive to quark masses (as long as $m < T$). Therefore linkage is a robust quantity above T_c.

U and D are not linked

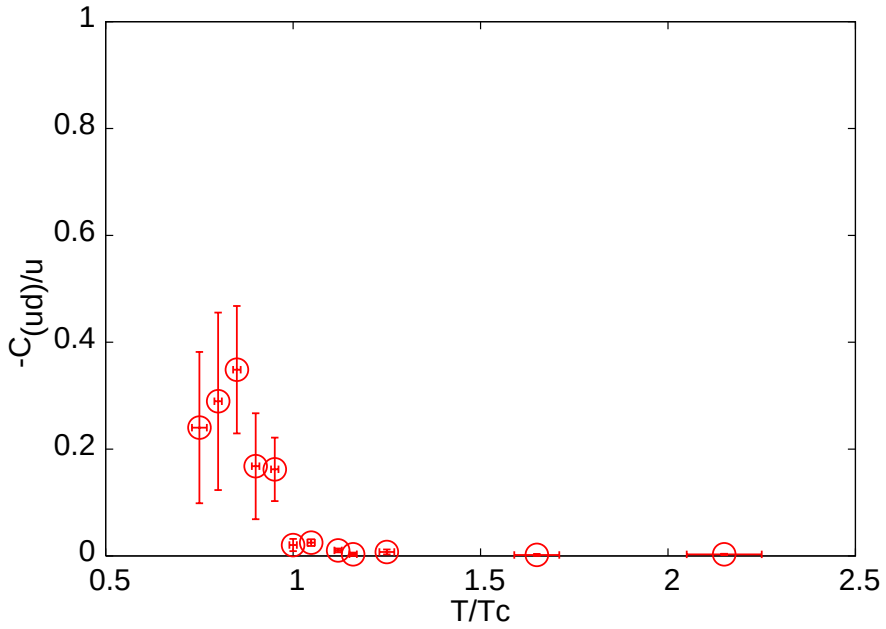

u and $\overline{d}$ can be carried by the same particle below T_c but not above T_c.

Strangeness is carried by quarks

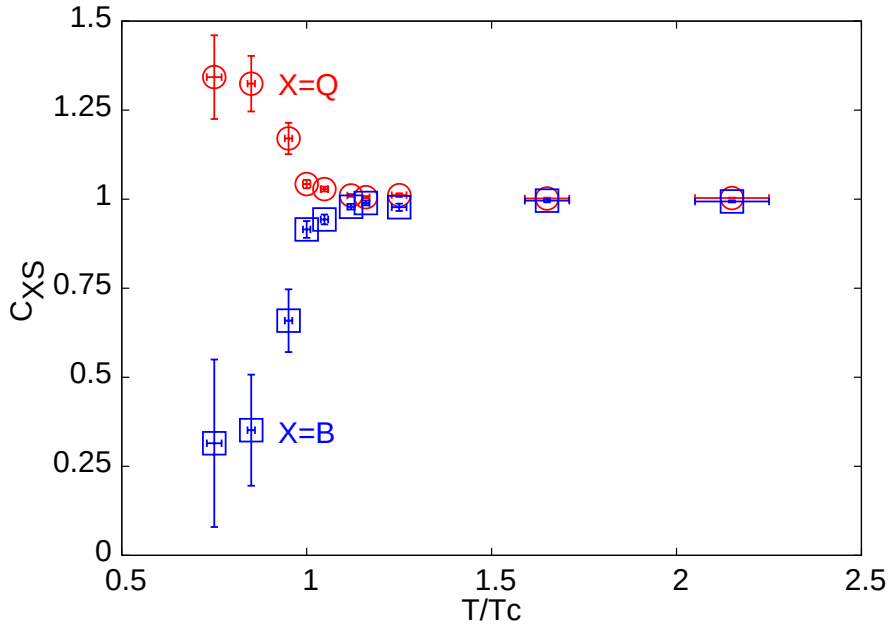

$C_{BS} = -3C_{(BS)|S}$ and $C_{QS} = 3C_{(QS)|S}$. Below T_c strange baryons are relatively heavy and therefore sparse in the plasma, but kaons are not so heavy. Above T_c: strange quarks.

Koch, Majumder, Randrup, PRL 95 (2005) 182301, Gavai and SG, PRD 73 (2006) 014004

Screening correlators with overlap quarks

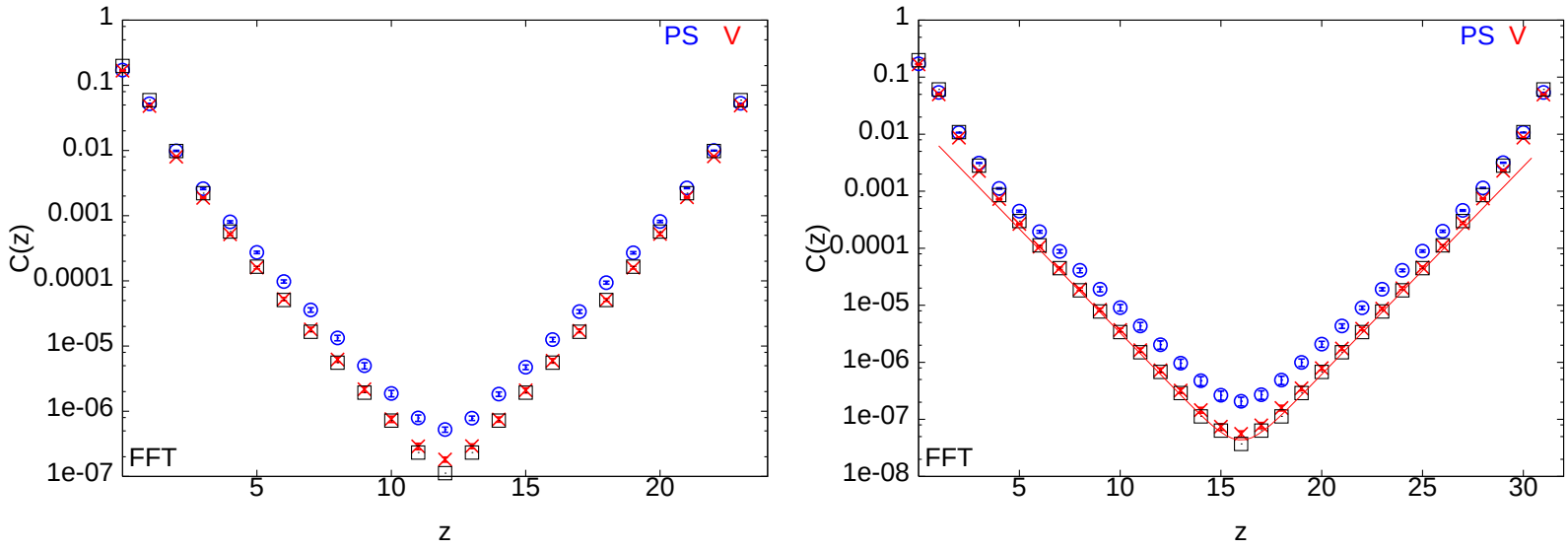

$N_s = 4/T$; $a = 1/6T$ and $a = 1/8T$; overlap. Fit to Bose gas good only over limited range of z, so screening masses not quoted. Vector correlator close to ideal gas of quarks.

Pseudoscalar correlator badly described by ideal quark gas at long distances and by Bose gas at short distances. Does not seem to be a finite lattice spacing artifact. Gavai, SG, Lacaze

Screening correlators in momentum space

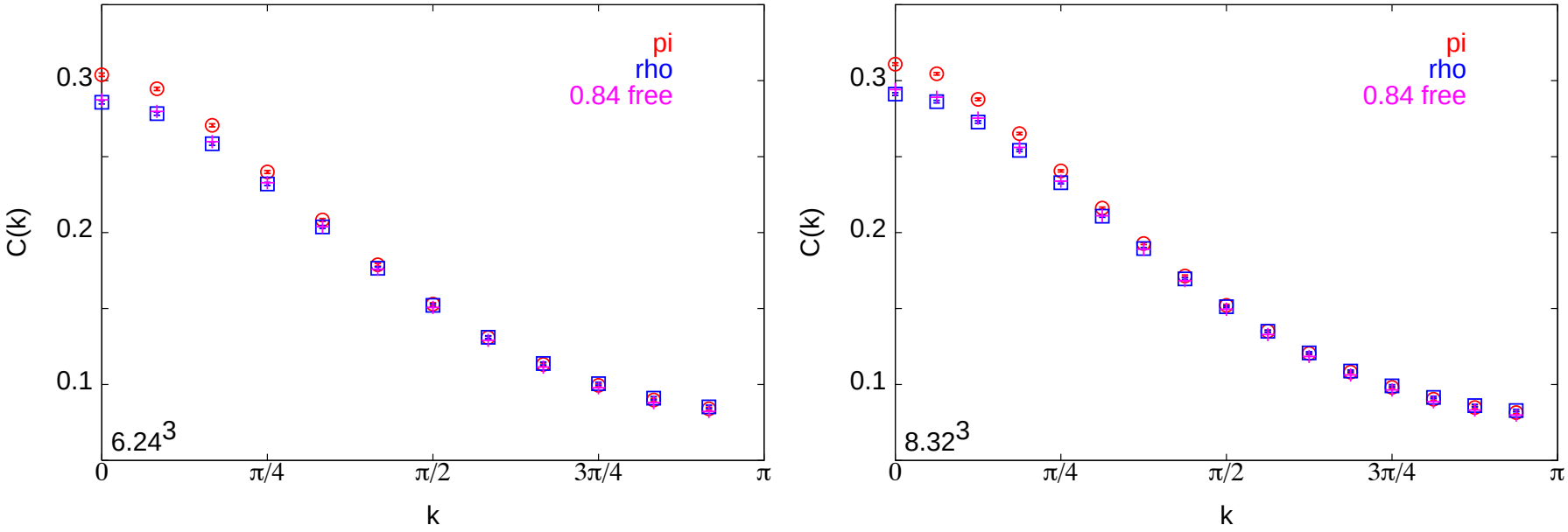

Vector screening correlator roughly compatible with ideal quark gas upto overall normalization. $\chi^2/\mathrm{D}OF \approx 3$, implying shape change is a small effect but definite. Try weak coupling expansion?

Pseudoscalar is definitely different at small momentum, but agrees at large momentum.

Lattice spacing effects in momentum space correlators

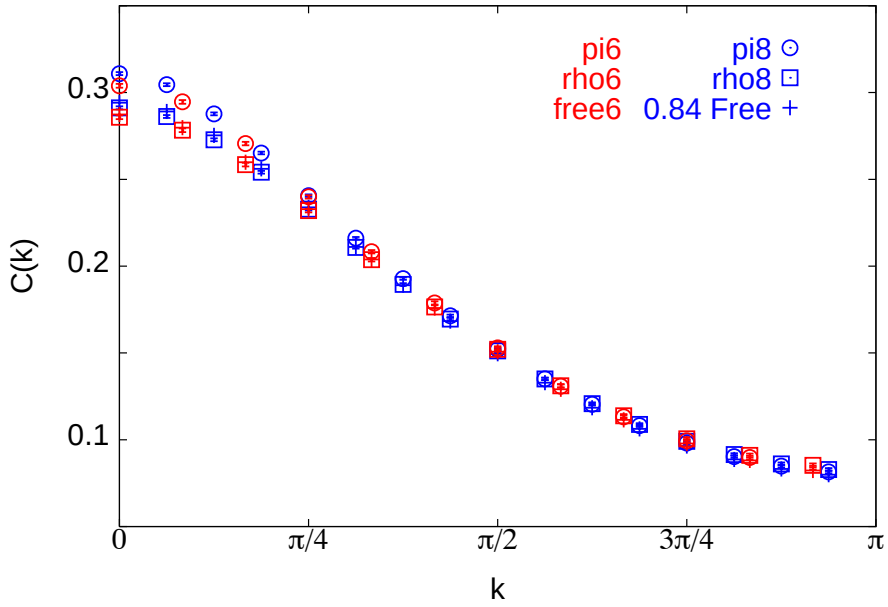

Lattice spacing effects? Some generic dependence, but nothing in $C_\pi(0)/C_\rho(0)$.

Summary of 2nd part

1. Immediately above the crossover, quark-like quasi-particles can be observed in the QCD plasma. Linkage is usually visible in experiments— called particle id, when single particles can be tagged in detector. In plasma need to use linkage as defined.

2. Screening masses with overlap quarks give extra indications about the nature of the excitations.